ELSEVIER

Chemical Physics 212 (1996) 381–391

Chemical Physics

An ab initio perturbed ion study of structural properties of TiO_2, SnO_2 and GeO_2 rutile lattices

A.C. Camargo [a], J.A. Igualada [b], A. Beltrán [b,*], R. Llusar [b], E. Longo [a], J. Andrés [b]

[a] *Department of Chemistry, Universidade Federal de Sao Carlos, 131560 Sao Carlos, Brazil*
[b] *Department of Experimental Sciences, Universitat Jaume I, Box 242, 12080 Castelló, Spain*

Received 12 April 1996

Abstract

This work describes a theoretical quantum mechanical study on TiO_2, SnO_2 and GeO_2 rutile structures in order to characterize the geometric, mechanical, thermodynamic and electronic properties of these systems. The doping processes of V^{4+} at the sixfold-coordinated site have been studied with the aim of determining the relative stability of pure and doped structures. Ab initio perturbed ion calculations with Slater-type orbitals for representing atomic centers and large cluster models have been used. Local geometry optimizations have been performed to determine the lattice energy, lattice parameters and bulk modulus, as well as the force constant and vibrational frequencies (ν) of the breathing vibrational modes, a_{1g}, in the sixfold-coordinated site. Numerical results are analyzed and compared with experimental data, the geometrical distances obtained by computer simulation being in agreement with the reported experimental values. The difference in energy for the substitution of Ti^{4+}, Sn^{4+} and Ge^{4+} for V^{4+} in TiO_2, SnO_2 and GeO_2, respectively is very dependent on the method used to represent these doping processes. The TiO_2, SnO_2 lattices show a decrease in the ν value from the pure to the doped structure while a opposite trend is obtained for the GeO_2 structure. The validity of the methodology is discussed.

1. Introduction

TiO_2, SnO_2 and GeO_2 rutile-type structures have been the subject of numerous experimental works since they are interesting materials of technological importance, i.e. in catalytic chemistry, electrochemistry and other material sciences [1–9]. The study of these structures add to their intrinsic interest, the fact that they constitute surfaces whose study can provide a proper understanding of their behavior at an atomic scale.

The theoretical investigation of the chemical and physical nature of solids requires the knowledge of their properties obtained with appropriate methods [10,11]. Three methodologies have been used to carry out theoretical studies on solid state chemistry [12]: simulation techniques (Monte Carlo, molecular dynamics, etc.), local density approximation (LDA) and electronic structure techniques. Owing to recent advances in computer power, reliable and accurate ab initio calculations on the latter kind of methods would be very useful since this information is com-

* Corresponding author. Fax: +34 64 345654.

PII S0301-0104(96)00228-5

plementary to that obtained using different available theoretical and experimental techniques. In particular, the ab initio Perturbed Ion (aiPI) method, has been successfully applied to the calculation of the electronic structure of different systems like halides [13], hydrides [14], binary oxides [15,16], zircon [17], different oxo- and fluoroperovskites [18,19], garnet [20], and spinel [21] lattices.

Following recent achievements in applying this methodology to the understanding of some of the physical and chemical properties relevant to the condensed matter, in this work which can be considered a continuation of previous papers [16–21] we have carried out a step beyond studying rutile-type crystals having an unclear ionic character. In spite of numerous theoretical studies on rutile systems carried out by extended Hückel [22], semiempirical [23], density functional with LDA approximation and with Hartree–Fock approximations [24–33], features such a lattice parameters, bulk modulus, electronic properties, force constants and vibrational frequencies associated with normal modes are far from being theoretically established.

The following aspects are considered in this paper. (i) Evaluation of crystal properties such as lattice parameters, equilibrium distances, lattice energy and bulk modulus of TiO_2, SnO_2 and GeO_2 rutile structures. (ii) Calculation of the electronic structure and equilibrium geometry around the impurity center (V^{4+}). (iii) Evaluation of defect energy associated with the doping process at sixfold-coordinated site. (iv) Evaluation of force constant and vibrational frequencies associated to local distortion in the pure and doped structures. (v) Comparison among our results, previous theoretical and experimental data.

The layout of this paper is as follows: the method and model are summarized in Section 2. The results and discussion are presented in Section 3. A short section of conclusions closes this paper.

2. Method and model

2.1. The aiPI method

The aiPI method [34,35], provides an adequate quantum-mechanical treatment of the atom in the lattice structure and offers a computationally tractable approach to the analysis of the electronic structure in solids. This method is essentially based on an improved formulation [36–40] of the general theory of electronic separability (TES) and gives detailed information on the ionic wave functions and the microscopic interactions determining the relative stability of pure and doped structures. In the aiPI method one can study local defects in terms of clusters whose size and characteristics properly simulate the crystal environment and the way it reacts to the presence of impurity ions [41]. A detailed description of the method can be found in the paper of Pueyo et al. [34].

2.2. Structural details and models

TiO_2, SnO_2 and GeO_2 crystallize with the bulk rutile structure (space group $P4_2/mnm$) [1,42]. In Fig. 1 a schematic representation of the lattice is depicted. The atom coordinates are M: (0,0,0),(1/2,1/2,1/2) and O: $\pm(x,x,0),\pm(1/2+x,1/2-x,1/2)$, M being Ti, Sn or Ge. The structure consists of chains of MO_6 octahedra and each pair shares opposite edges. Each metal atom is surrounded octahedrally by six oxygen atoms, whereas

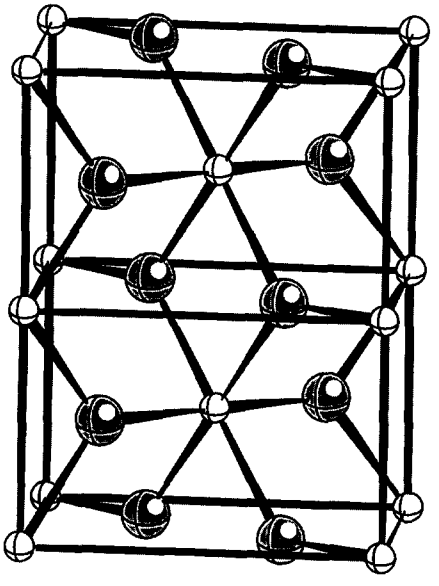

Fig. 1. Rutile structure (two unit cells), light grey spheres represent oxygen atoms and white spheres the metal atoms.

each oxygen is surrounded by three metal atoms arranged as corners of an equilateral triangle. The structure has a 6:3 coordination. Each octahedron is not regular, showing a slight orthorhombic distortion and is in contact with ten neighbor octahedra, two sharing edge oxygen pairs and eight sharing corner oxygen ions [22,30].

First, aiPI calculations for pure infinite crystals have been carried out, applying periodic boundary conditions. Second, in order to study the local geometry, we have self-consistently computed the electronic structure of six large clusters: $Ti_{32}O_{64}$, $VTi_{31}O_{64}$, $Sn_{32}O_{64}$, $VSn_{31}O_{64}$, $Ge_{32}O_{64}$ and $VGe_{31}O_{64}$ to avoid size effects. For these large clusters, the wavefunctions and effective potentials that describe the lattice environment were obtained from previous aiPI calculations for the pure infinite cluster, showing that at this size level the calculated results are independent of the number of atoms representing the crystal. These clusters are formed by a metal ion at the origin and nineteen successive shells of ions symmetrically distributed around it.

The geometry of rutile-type structures was first optimized by varying the positional parameter and cell length, and calculating the effective energy, until a minimum was found. Geometry optimization was achieved by means of the POWELL subroutine [43].

Parameters "a" and "x" were optimized, while parameters "b" and "c" were kept dependent of "a" by constrain ("b" was set equal to "a" and "c" was obtained by the quotient of a/c fixed at the experimental value [1]). Local optimizations have been performed on the first and second coordination spheres around the cluster origin. The first shell is composed of six oxygen atoms octahedrally distorted arranged around the origin and the second shell of 10 metal atoms decahedrally distorted distributed around the origin, as seen in Fig. 2. The distance from the first and second shell to the origin has been varied stepwise until a minimum in the effective energy has been reached. The optimization has been carried out

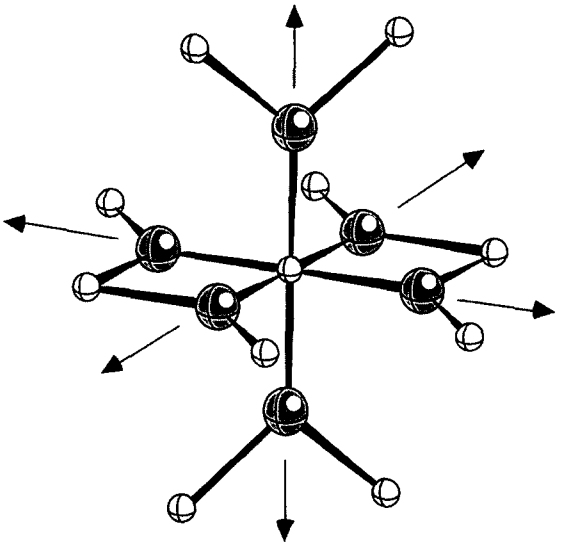

Fig. 2. Structure of the first and second shell of atoms around the origin of cluster, light grey spheres represent oxygen atoms and white spheres the metal atoms. Radial displacements $\delta_{a_{1g}}$ associated with the a_{1g} vibrational mode are indicated in the figure.

Table 1
Orbital energies (au), orbital exponents and expansion coefficients for oxygen: $1s^2 2s^2 2p^6 \rightarrow {}^1S$ (this notation is taken from Clementi and Roetti [42])

		1S	2S			2P
orbital energy		−20.067519	−0.952423			−0.226454
n,λ	orbital exponent	ϕ(1s) expansion coefficient	ϕ(2s) expansion coefficient	n,λ	orbital exponent	ϕ(2p) expansion coefficient
1S	13.425500	0.03836452	−0.00703852	2P	7.820440	0.03132279
1S	7.614670	0.93704423	−0.19954901	2P	3.429750	0.16693879
2S	6.314910	0.03527495	−0.10388060	2P	1.743990	0.84847486
2S	3.212690	0.00356408	0.43031358	2P	0.863930	0.02889720
2S	1.750760	0.00026049	0.69659993	2P	0.408310	−0.04671877

expanding or contracting the two shells by the same factor.

A vibrational analysis for the breathing radial mode at octahedral site for the pure and doped structures has been carried out. The optimization schemes, and the numerical calculations of derivatives were computed by specific driver programs.

2.3. Basis sets

Large STO basis sets were used to describe the ions: (5s5p) for O^{2-}, (7s5p) for Ti^{4+}, (8s6p5d) for Sn^{4+}, (8s6p5d) for Ge^{4+} and (8s6p5d) for V^{4+} [44]. The wave functions and effective potentials that describe the lattice environment on each cluster were obtained from a previous aiPI calculation for the pure, infinite cluster. The optimization of these basis sets was done in order to minimize the total energy while maintaining SCF stability. The description of orbitals with s, p and d symmetry for all ions are listed in Tables 1–5.

The Madelung potential, responsible for the largest part of the interaction energies, has been analytically integrated. Layer by layer Ewald summation techniques were used to accurately sum long range Coulomb potential contributions.

The quantum mechanical contributions to the interaction energies have been considered for a large number of neighbor shells until a convergence of 10^{-6} hartree is achieved in the effective energy of the clusters. The effective energy includes correlation estimated by means of the unrelaxed Coulomb–Hartree–Fock formalism [45]. The term unrelaxed is used because the aiPI wavefunctions are not affected by this correction.

3. Results and discussion

3.1. Lattice parameters and bulk modulus

Optimization of the rutile-type structures yields the lattice energy and lattice parameters reported in

Table 2
Orbital energies (au), orbital exponents and expansion coefficients for titanium: $1s^2 2s^2 3s^2 2p^6 3p^6 \rightarrow {}^1S$

		1S	2S	3S
orbital energy		−183.669012	−21.875539	−3.155969
n,λ	orbital exponent	ϕ(1s) expansion coefficient	ϕ(2s) expansion coefficient	ϕ(3s) expansion coefficient
1S	21.649900	0.95311047	−0.29247239	0.10771729
1S	34.754700	0.02432473	−0.00185053	0.00098621
2S	8.826350	0.00738927	1.03796471	−0.42691438
2S	18.961800	0.02759745	−0.14672092	0.06137640
3S	4.900940	0.00239178	0.00648469	0.50498386
3S	3.432120	−0.00089063	0.00044275	0.72393701
3S	7.702770	−0.00503138	0.10570226	−0.22435456
		2P	3P	
orbital energy		−18.238963	−2.040363	
n,λ	orbital exponent	ϕ(2p) expansion coefficient	ϕ(3p) expansion coefficient	
2P	10.120700	0.67905769	−0.25363080	
2P	16.909700	0.05118642	−0.01642675	
3P	4.238420	0.01346287	0.56165262	
3P	2.950110	−0.00371473	0.54887580	
3P	8.413080	0.31835281	−0.14926906	

Table 6, which come close to experimental data [1,42] and semiempirical calculations by Lunell et al. [23] of TiO_2 clusters render a Ti–O distance in the range 187–224 pm.

Isotropic volume changes were used to determine the bulk modulus, B, which can be calculated by changing the cell edge and finding the resulting lattice energy. B and its pressure derivative, B', of TiO_2, SnO_2 and GeO_2 have been estimated using the Birch–Murnaghan third-order [46] equation of state. The calculated B and B' (in parentheses) are: 200.07 GPa (4.00), 138.42 GPa (4.00) and 205.17 GPa (3.86) for the TiO_2, SnO_2 and GeO_2 lattices, respectively. These values are lower than the experimental results reported by Hazen and Finger [47] (see Table 6). We have point out [16,21] that the aiPI method underestimates the B values while other calculations on rutile systems based in LDA [27] or periodic Hartree–Fock [48] methods tend to overestimate these parameters. The rutile structures are less

Table 3
Orbital energies (au), orbital exponents and expansion coefficients for germanium: $1s^2 2s^2 3s^2 2p^6 3p^6 3d^{10} \rightarrow {}^1S$

		1S	2S	3S
orbital energy		−405.290537	−52.159735	−7.168860
n,λ	orbital exponent	ϕ(1s) expansion coefficient	ϕ(2s) expansion coefficient	ϕ(3s) expansion coefficient
1S	29.297200	−0.95337659	0.37403767	0.13318153
1S	43.944100	−0.09346152	−0.01372411	0.00080708
2S	24.393000	0.07372108	0.13330494	0.08721452
2S	13.034400	−0.04367562	−1.19564706	−0.57677077
3S	11.657200	0.03150942	0.04552661	−0.08804216
3S	7.074610	−0.01880468	−0.05737599	0.72745018
3S	4.603680	0.02825222	0.07225488	0.67962734
3S	4.153600	−0.01933294	−0.04921396	−0.20464357
		2P	3P	
orbital energy		−46.254063	−5.152537	
n,λ	orbital exponent	ϕ(2p) expansion coefficient	ϕ(3p) expansion coefficient	
2P	12.351300	0.86639529	−0.37833847	
2P	20.284500	0.18022675	−0.05666778	
3P	10.106400	−0.05816339	−0.01505665	
3P	6.938750	0.04145151	0.70495452	
3P	4.155380	−0.00954397	0.46581771	
3P	1.888010	0.00176520	−0.01948754	
		3D		
orbital energy		−1.628567		
n,λ	orbital exponent	ϕ(3d) expansion coefficient		
3D	4.921590	0.45032022		
3D	13.925700	0.04275963		
3D	7.927710	0.31725132		
3D	2.898990	0.34178994		
3D	1.910890	−0.02813214		

compressible than other structures calculated by us, such as pyrope, grossularite, yttrium aluminum garnet [20] and ceria [16].

3.2. Energetics

The defect reaction energies [17,49] of V_M centers in MO_2 (M = Ti, Sn and Ge) have been theoretically evaluated by analyzing the free energy of the process

$$[M^{4+}\text{-cluster}]{:}MO_6 + V^{4+} \leftrightarrow [V^{4+}\text{-cluster}]{:}MO_6 + M^{4+}. \quad (1)$$

As long as the thermal effects are negligible the substitution is governed by the internal energy, which can be obtained in our quantum-mechanical calculation as

$$E_{\text{left}} = E_{\text{total}}(M^{4+}\,\text{cluster:lattice}) - E_{\text{vac}}(V^{4+}), \quad (2)$$

$$E_{\text{right}} = E_{\text{total}}(V^{4+}\,\text{cluster:lattice}) - E_{\text{vac}}(M^{4+}), \quad (3)$$

where $E_{(\text{left})}$ and $E_{(\text{right})}$ denote the left- and right-hand sides of Eq. (1), respectively, and E_{vac} is the energy of the free ion. The difference between the

Table 4
Orbital energies (au), orbital exponents and expansion coefficients for tin: $1s^2 2s^2 3s^2 4s^2 2p^6 3p^6 4p^6 3d^{10} 4d^{10} \rightarrow {}^1S$

		1S	2S	3S	4S
orbital energy		−1041.149390	−156.890234	−31.499354	−5.386310
n,λ	orbital exponent	ϕ(1s) expansion coefficient	ϕ(2s) expansion coefficient	ϕ(3s) expansion coefficient	ϕ(4s) expansion coefficient
1S	51.222400	0.87212250	0.02957294	0.00970518	−0.00250420
1S	34.308200	0.14927936	0.50890212	0.22993885	−0.10280976
2S	24.726100	−0.08581060	−0.18053803	0.40432077	−0.18641823
2S	21.525400	0.06982913	−1.02593929	−1.15363753	0.52311498
3S	15.574800	−0.00965038	−0.04400956	0.01614140	0.07045799
3S	11.078900	0.00360540	0.00665806	1.18223394	−0.79052797
4S	6.400880	−0.00068215	−0.00070894	0.02893983	0.84429141
4S	4.372570	0.00029672	0.00035802	−0.00567430	0.36976150
		2P	3P	4P	
orbital energy		−146.404601	−27.112444	−3.850294	
n,λ	orbital exponent	ϕ(2p) expansion coefficient	ϕ(3p) expansion coefficient	ϕ(4p) expansion coefficient	
2P	32.557600	−0.13253266	−0.02930681	0.00861155	
2P	21.410800	−0.86959329	−0.48430397	0.21133723	
3P	11.365600	−0.03234285	0.96872612	−0.43835794	
3P	8.234690	0.02139076	0.16188187	−0.25577874	
4P	6.839780	−0.00674997	0.01050663	0.64536162	
4P	4.422400	0.00125395	−0.00073357	0.62688699	
		3D	4D		
orbital energy		−19.070234	−1.245984		
n,λ	orbital exponent	ϕ(3d) expansion coefficient	ϕ(4d) expansion coefficient		
3D	18.024800	−0.21672673	−0.08242711		
3D	10.383800	−0.79487850	−0.30224374		
4D	6.404450	−0.05812773	0.37338942		
4D	4.053700	0.01297071	0.60033064		
4D	2.541470	−0.00320322	0.18125106		

Table 5
Orbital energies (au), orbital exponents and expansion coefficients for vanadium: $1s^2 2s^2 3s^2 2p^6 3p^6 3d^1 \rightarrow {}^2D$

		1S	2S	3S
orbital energy		−203.580464	−26.005786	−5.148746
n,λ	orbital exponent	ϕ(1s) expansion coefficient	ϕ(2s) expansion coefficient	ϕ(3s) expansion coefficient
1S	22.980300	−0.94833732	0.29873410	0.11000297
1S	36.372800	−0.01612419	−0.00351275	−0.00057130
2S	19.363600	−0.04697577	0.15933059	0.06867591
2S	9.290610	0.00141096	−1.05907759	−0.44277348
3S	8.185360	−0.00218350	−0.08622193	−0.21150782
3S	5.310870	0.00208236	−0.02149877	0.41803442
3S	3.798410	−0.00166298	0.01077974	0.71787083
3S	3.026610	0.00066930	−0.00456805	0.08970481
		2P	3P	
orbital energy		−22.149912	−3.947796	
n,λ	orbital exponent	ϕ(2p) expansion coefficient	ϕ(3p) expansion coefficient	
2P	10.458300	0.67381934	−0.25018636	
2P	16.758400	0.07010620	−0.02513646	
3P	8.988800	0.29442905	−0.15557277	
3P	4.822490	0.03170436	0.41730139	
3P	3.568050	−0.02674384	0.29021289	
3P	3.097500	0.01289621	0.41276350	
		3D		
orbital energy		−2.408378		
n,λ	orbital exponent	ϕ(3d) expansion coefficient		
3D	2.837240	0.52538561		
3D	9.995020	0.03109802		
3D	4.817780	0.33798275		
3D	2.188270	0.17308485		
3D	6.305890	0.02472615		

Table 6
Lattice parameters a (pm), c (pm), x; lattice energy E_{latt} (kJ mol^{-1}); bulk modulus B (GPa) and its pressure derivative B'

		a [a]	c [a]	x [a]	E_{latt}	B [b]	B' [b]
TiO_2	exp	459.4	295.9	0.306	−7381.9	216	7
	calc	462.8	298.6	0.306	−7441.1	200.07	4.00
SnO_2	exp	473.7	318.5	0.307	−7655.3	218	7
	calc	447.8	300.9	0.308	−7744.4	138.42	4.00
GeO_2	exp	439.5	2.860	0.307	−8735.1	258	7
	calc	410.9	267.1	0.307	−8879.7	205.17	3.86

[a] Experimental values taken from Refs. [1,40].
[b] Experimental values taken from Ref. [45].

two former energies yields the substitutional energy, which in our case measures the stability of V^{4+} in the lattice. Although the total energy of the crystal is in general difficult to calculate, it can be estimated in a simplified way by assuming that the system is divided into the impurity center, the cluster surrounding the defect, and the remainder of the crystal. Accordingly the total energy for the pure and doped structures can be written as

$$E_{\text{total}}(M^{4+}\text{cluster:lattice}) = E_{\text{eff}}(M^{4+}\text{:cluster:M}) + E_{\text{rest}}, \quad (4)$$

$$E_{\text{total}}(V^{4+}\text{:cluster:lattice}) = E_{\text{eff}}(V^{4+}\text{:cluster:V}) + E'_{\text{rest}}. \quad (5)$$

The defect reaction or relative substitutional energy, ΔE_{def}, would thus be given as

$$\Delta E_{\text{def}}(V_M) = E_{\text{eff}}(V^{4+}\text{:cluster}) - E_{\text{eff}}(M^{4+}\text{:cluster}) + E_{\text{vac}}(M^{4+}) - E_{\text{vac}}(V^{4+}). \quad (6)$$

E_{eff} denotes the effective energy of the cluster in the lattice and E_{rest} the energy associated to the rest of the crystal. In the above equations it is assumed that E_{rest}, which labels a quantity other than the effective energy of the cluster, remains unchanged upon substitution, i.e. $E_{\text{rest}} = E'_{\text{rest}}$. This is due to the fact that the effective energy of the cluster contains all the components of the total energy in which the wave functions of the substituted center and the ions in the cluster directly participate. This approximation should be more adequate for isovalent impurities as the cluster size grows.

The defect reaction or relative substitution energies (ΔE_{def}) corresponding to the V^{4+} substitution in the host material are listed in Table 7. The ΔE_{def} corresponding to V^{4+} substitution in TiO_2 and SnO_2 lattices are energetically favored by -187.7 and -7.0 kJ mol^{-1}, respectively. This result is in agreement with a experimental study based on electron spin resonance spectra of vanadium doped rutile [50]. In the GeO_2 cluster ΔE_{def} has a positive value ($+735.9$ kJ mol^{-1}), in accordance with our previous calculation [49] in which Ge^{4+} substitution by V^{4+} is disfavored. These results are presented for calculations in which the geometrical parameters of the cluster have been optimized.

An alternative estimation of the energy associated with the doping process can be obtained assuming a simple direct reaction between the solid reactants: VO_2(s) and MO_2(s). The process can be schematically represented as

$$VO_2(s) \leftrightarrow V^{4+}(g) + 2O^{2-}(g), \quad (a)$$

$$V^{4+}(g) + xMO_2(s) \leftrightarrow VM_{x-1}O_{2x}(s) + M^{4+}(g), \quad (b)$$

$$M^{4+}(g) + 2O^{2-}(g) \leftrightarrow MO_2(s). \quad (c)$$

Table 7
Cluster stoichiometry, optimized and experimental bond distances, force constants, vibrational frequencies, defect, ΔE_{def}, and direct solid state, ΔE, energies for pure and doped structures

	TiO_2		SnO_2		GeO_2	
	pure	doped	pure	doped	pure	doped
cluster stoichiometry	$Ti_{32}O_{64}$	$VTi_{31}O_{64}$	$Sn_{32}O_{64}$	$VSn_{31}O_{64}$	$Ge_{32}O_{64}$	$VGe_{31}O_{64}$
d_{opt} [M–O] (pm) 4×	210.0	210.9	207.1	207.1	187.7	187.7
d_{exp} [M–O] (pm) 4×	199.4	–	205.2	–	187.0	–
d_{opt} [M–O] (pm) 2×	214.2	215.2	208.5	208.5	191.4	191.4
d_{exp} [M–O] (pm) 2×	198.8	–	205.6	–	191.0	–
force constant (N m^{-1})	58402	55586	67251	65565	55972	80567
vib. frequency (cm^{-1})	3214	3135	3449	3405	3146	3775
ΔE_{def} (kJ mol^{-1})	–	−187.7	–	−7.0	–	+735.9
ΔE (kJ mol^{-1})	–	+151.0	–	−379.2	–	−376.8

Addition of steps (a), (b) and (c) yields the global reaction

$$VO_2(s) + xMO_2(s) \leftrightarrow VM_{x-1}O_{2x}(s) + MO_2(s). \quad (7)$$

The energy change, ΔE, associated with the reaction (7) can be calculated from the following expression:

$$\Delta E = \Delta E_{def} + \Delta E_{latt}, \quad (8)$$

where

$$\Delta E_{latt} = E_{latt}(MO_2) - E_{latt}(VO_2) \text{ for reaction (7)},$$

E_{latt} being the lattice energy and ΔE_{def} the defect reaction energy.

Table 6 lists the lattice energies E_{latt} for the rutile-type optimized geometries and the E_{latt} of VO_2 was calculated in a previous work [49]. The energy variations ΔE, reported in Table 7, calculated for the direct solid state reaction corresponding to V^{4+} substitution into TiO_2, SnO_2 and GeO_2 are +151.0, −379.2 and −376.8 kJ mol^{-1}, respectively.

3.3. Optimized local geometries

The optimized bond distances for pure and doped rutile-type structures are also presented in Table 7. These distances have been optimized by minimizing the cluster energies as reported in Section 2.

Optimization of the titanium centered $Ti_{32}O_{64}$ cluster yields a local geometry around Ti, d(Ti–O) = 210.0 pm (4 ×) and d(Ti–O) = 214.2 pm (2 ×), which shows a 5.32% and 7.75% expansion with regard to the reported experimental distance. The optimal geometries for the equivalent V^{4+} doped centered cluster ($VTi_{31}O_{64}$) show an increase in the origin–oxygen distance of 1.0 pm (for both distances) with regard to the pure structure optimized Ti–O distances.

Optimization of the tin centered $Sn_{32}O_{64}$ cluster yields a local geometry around Sn, d(Sn–O) = 207.1 pm (4 ×) and d(Sn–O) = 208.5 pm (2 ×), which shows a 0.93% and 1.41% expansion with regard to the reported experimental distance. The optimal geometries for similar V^{4+} doped centered cluster ($VSn_{31}O_{64}$) show no increase in the origin–oxygen distance with regard to the pure structure optimized Sn–O distances.

Optimization of the germanium centered $Ge_{32}O_{64}$ clusters yields a local geometry around Ge, d(Ge–O) = 187.7 pm (4 ×) and d(Ge–O) = 191.4 pm (2 ×), which shows a 0.37% and 0.21% expansion with regard to the reported experimental distance. The optimal geometries for the equivalent V^{4+} doped centered cluster ($VGe_{31}O_{64}$) show no increase in the origin–oxygen distance with regard to the pure structure optimized Ge–O distances.

3.4. Vibrational frequencies

Vibrational frequencies of breathing normal modes for the pure and doped structures have been determined approximately by calculating the cluster effective energy E_{eff} as a function of small a_{1g} symmetry adapted displacements, $\delta_{a_{1g}}$, of the first coordination sphere of oxygen ions around the origin. These displacements, defined by Fig. 2, have been treated as approximate normal modes, and the frequency ν has been calculated from

$$\nu = \frac{1}{2\pi}\sqrt{\frac{K}{m}} \text{ with } K = \left(\frac{\partial^2 E_{eff}}{\partial Q^2}\right)_0,$$

where m is the reduced mass and the symmetry adapted for octahedral coordinate $\delta_{a_{1g}}$ site Q is

$$Q_{a_{1g}} = \delta_{a_{1g}}\sqrt{6}.$$

The calculated vibrational frequencies for the pure and V^{4+} doped structures are listed in Table 7. In TiO_2 and SnO_2 cases the doping process produces a decrease in the force constants and consequently in the vibrational frequencies associated with the approximate breathing normal mode. This result is similar to recent reported data for zircon [17] and $ZrGeO_4$ [49] structures.

4. Conclusions

Embedded cluster calculations on pure and V^{4+} doped TiO_2, SnO_2 and GeO_2 lattices have proved to be an appropriate procedure for evaluating defect reaction energies, geometry distortions and changes in vibrational frequencies originating from the doping process.

The results of the present study can be summarized as follows.

1. The calculated lattice parameters and internal atomic coordinates agree reasonably with experimental data for pure structures. The doping process produces a expansion, 1 pm, for the first shell of oxygen centers for TiO_2 structure while SnO_2 and GeO_2 lattices remain invariant.
2. Bulk modulus are 200.07, 138.42 and 205.17 GPa for the TiO_2, SnO_2 and GeO_2 lattices, respectively.
3. The energies required to substitute Ti^{4+}, Sn^{4+} and Ge^{4+} for V^{4+} into the TiO_2, SnO_2 and GeO_2 lattices in a straightforward solid state reaction, ΔE, are $+151.0$, -379.2 and -376.8 kJ mol^{-1}, respectively. However, the energetic results obtained by means of defect energy, ΔE_{def}, are -187.7, -7.0 and $+735.9$ kJ mol^{-1}, respectively.
4. The TiO_2, SnO_2 lattices show a decrease in the ν value from the pure to the V^{4+} doped structure while a opposite trend is obtained for the GeO_2 structure.

Acknowledgements

We are most indebted to V. Luaña and A. Martín-Pendás for sending us their latest version of the aiPI method and to Centre d'Informàtica at Universitat Jaume I and Centro Nacional de Processamento de Alto Desempenho (CENAPAD-SP) for providing us with multiple computing facilities.

References

[1] V.W.H. Baur, Acta Crystallogr. 9 (1956) 515.
[2] Y. Nakato, H. Ogawa, K. Morita and H. Tsubomura, J. Phys. Chem. 90 (1986) 6210.
[3] D. Kohl, Sens. Actuators 18 (1989) 71.
[4] F. Okada, A. Satsuma, A. Miyamoto, T. Hattori and Y. Murakami, J. Phys. Chem. 94 (1990) 5900; K.M. Schindler and M. Kunst, J. Phys. Chem. 94 (1990) 8222.
[5] N. Nicoloso, Ber. Bursenges. Phys. Chem. 94 (1990) 731.
[6] K. Siroki and J. Jiresová, Talanta 41 (1994) 1735; A. Hagfeldt, B. Didriksson, T. Palmqvist, H. Lindström, S. Södergren, H. Rensmo and S.-E. Lindquist, Solar Energy Mater. Solar Cells 31 (1994) 481.
[7] G. Lassaletta, A. Fernández, J.P. Espinós and A.R. González-Elipe, J. Phys. Chem. 99 (1995) 1484; P. Maruthamuthu, D.K. Sharma and N. Serpone, J. Phys. Chem. 99 (1995) 3636; R. Dixon, R.E. Egdell and G. Beamson, J. Chem. Soc. Faraday Trans. 91 (1995) 3495.
[8] A.L. Linsebigler, G. Lu and J.T. Yates Jr., Chem. Rev. 95 (1995) 735.
[9] K.H. Liao and D.H. Waldeck, J. Phys. Chem. 99 (1995) 4569.
[10] J. Sauer, Chem. Rev. 363 (1989) 493; J. Sauer, Nature 363 (1993) 493.
[11] C.R.A. Catlow and G.D. Price, Nature 347 (1990) 243.
[12] C.R.A. Catlow, J.D. Gale and R.W. Grimes, J. Solid State Chem. 106 (1993) 13.
[13] V. Luaña and L. Pueyo, J. Mol. Struct. THEOCHEM 166 (1988) 215.
[14] V. Luaña and L. Pueyo, Phys. Rev. B 41 (1990) 3800.
[15] V. Luaña, F. Recio and L. Pueyo, Phys. Rev. B 42 (1990) 1791.
[16] J. Andrés and A. Beltrán, Chem. Phys. Letters 221 (1994) 249.
[17] A. Beltrán, A. Flores-Riveros, J.A. Igualada, G. Monrós, J. Andrés, V. Luaña and A. Martín-Pendás, J. Phys. Chem. 97 (1993) 2555; A. Beltrán, A. Flores-Riveros, J. Andrés, V. Luaña and A. Martín-Pendás, J. Phys. Chem. 98 (1994) 7741.
[18] J. Andrés, A. Beltrán, J.A. Igualada, R. Llusar and V. Moliner, J. Mol. Struct. THEOCHEM 330 (1995) 313.
[19] J. Andrés and A. Beltrán, J. Phys. Chem. 99 (1995) 8092.
[20] A. Beltrán, J. Andrés, J.A. Igualada and J. Carda, J. Phys. Chem. 99 (1995) 6493; J. Andrés, A. Beltrán and J.A. Igualada, J. Phys. Chem. Solids 56 (1995) 901.
[21] A. Beltrán, J.A. Igualada, R. Llusar and J. Andres, Intern. J. Quantum Chem. Symp. 29 (1995) 685.
[22] J.K. Burdett, Inorg. Chem. 24 (1985) 2244; J.K. Burdett, T. Hughbanks, G.J. Miller, J.W. Richardson Jr. and J.V. Smith, J. Am. Chem. Soc. 109 (1987) 3639.
[23] A. Hagfeldt, H. Siegbahn, S.-E. Lindquist and S. Lunell, Intern. J. Quantum Chem. 44 (1992) 477; N. Yu and J.W. Halley, Phys. Rev. B 49 (1995) 4768.
[24] K. Vos, J. Phys. C 10 (1977) 917.
[25] M.V. Ramana and D.H. Phillips, J. Chem. Phys. 88 (1988) 2637.
[26] B. Poumellec, P.J. Durham and G.Y. Guo, J. Phys. Condens. Matter 3 (1991) 8195.
[27] K.M. Glassford and J.R. Chelikowsky, Phys. Rev. B 46 (1992) 1284.
[28] B. Silvi, P. d'Arco and M. Causà, J. Chem. Phys. 93 (1990) 2637.
[29] B. Silvi, N. Fourati, R. Nada and R.A. Catlow, J. Phys. Chem. Solids 52 (1991) 1005.
[30] A. Fahmi, C. Minot, B. Silvi and M. Causà, Phys. Rev. B 47 (1993) 11717.
[31] A. Hagfeldt, S. Lunell and H. Siegbahn, Intern. J. Quantum Chem. 49 (1994) 97.
[32] M. Ramamoorty, D. Vanderbilt and R.D. King-Smith, Phys. Rev. B 49 (1994) 16721.

[33] Xu Wei-Xing, K.D. Shierbaum and W. Goepel, J. Solid State Chem. 121 (1996) 301.
[34] V. Luaña, M. Flórez, E. Francisco, A. Martín-Pendás, J.M. Récio, M. Bermejo and L. Pueyo, in: Cluster models for surface and bulk phenomena, eds. G. Pacchioni, P.S. Bagus and F. Parmigiani (Plenum Press, New York, 1992) p. 605.
[35] V. Luaña, A. Martin-Pendás, J.M. Recio, E. Francisco and M. Bermejo, Comput. Phys. Commun 77 (1993) 107.
[36] R. McWenny, Proc. Roy. Soc. London A 253 (1959) 242.
[37] S. Huzinaga and A.A. Cantu, J. Chem. Phys. 55 (1971) 5543.
[38] S. Huzinaga, D. Willians and A.A. Cantu, Advan. Quantum Chem. 7 (1973) 1987.
[39] V. Bonifacic and S. Huzinaga, J. Chem. Phys. 76 (1982) 2537.
[40] Y. Sakai and S. Huzinaga, J. Chem. Phys. 82 (1985) 270.
[41] V. Luaña and M. Flórez, J. Chem. Phys. 97 (1992) 6544.
[42] A. Wold and K. Dwight, Solid state chemistry: synthesis, structure and properties of selected oxides and sulfides (Chapman and Hall, New York, 1993).
[43] M.J.D. Powell, Numerical methods for non linear algebraic equations (Gordon and Breach, London, 1970).
[44] E. Clementi and C. Roetti, At. Data Nucl. Data Tables 14 (1974) 177.
[45] S.J. Chakravorty and E. Clementi, Phys. Rev. A 39 (1989) 2290.
[46] F.J. Birch, Geophys. Res. 57 (1952) 227.
[47] R.M. Hazen and L.W. Finger, J. Phys. Chem. Solids 42 (1981) 143.
[48] L.H. Jolly, B. Silvi and P. D'Arco, Eur. J. Mineral. 6 (1994) 7.
[49] J. Andrés, A. Beltrán and R. Llusar, Chem. Phys. Letters 236 (1995) 521.
[50] R.S. de Biasi, A.A.R. Fernandes and M.L.N. Grillo, J. Phys. Chem. Solids 55 (1994) 453.